

School closures, event cancellations, and the mesoscopic localization of epidemics in networks with higher-order structure

Guillaume St-Onge,^{1,2} Vincent Thibeault,^{1,2} Antoine Allard,^{1,2} Louis J. Dubé,^{1,2} and Laurent Hébert-Dufresne^{1,3,4}

¹Département de physique, de génie physique et d'optique,
Université Laval, Québec (Québec), Canada G1V 0A6

²Centre interdisciplinaire en modélisation mathématique,
Université Laval, Québec (Québec), Canada G1V 0A6

³Vermont Complex Systems Center, University of Vermont, Burlington, VT 05405

⁴Department of Computer Science, University of Vermont, Burlington, VT 05405

The COVID-19 epidemic is challenging in many ways, perhaps most obvious are failures of the surveillance system. Consequently, the official intervention has focused on conventional wisdom — social distancing, hand washing, etc. — while critical decisions such as the cancellation of large events like festivals, workshops and academic conferences are done on a case-by-case basis with limited information about local risks. Adding to this uncertainty is the fact that our mathematical models tend to assume some level of random mixing patterns instead of the higher-order structures necessary to describe these large events. Here, we discuss a higher-order description of epidemic dynamics on networks that provides a natural way of extending common models to interaction beyond simple pairwise contacts. We show that unlike the classic diffusion of standard epidemic models, higher-order interactions can give rise to mesoscopic localization, i.e., a phenomenon in which there is a concentration of the epidemic around certain substructures in the network. We discuss the implications of these results and show the potential impact of a blanket cancellation of events larger than a certain critical size. Unlike standard models of delocalized dynamics, epidemics in a localized phase can suddenly collapse when facing an intervention operating over structures rather than individuals.

I. INTRODUCTION

Classic disease models did the impossible in reducing the complexity of epidemics — shaped by complex social, biological and political forces — to simple processes that provide useful insights. In fact, many of the key results of these models provide the foundation for our current understanding and forecasting of novel emerging epidemics [1–3]. The reduction of the complex to the simple is perhaps best embodied by the attention given to the basic reproduction number R_0 of an outbreak. In one quantity, R_0 combines properties of the population, pathogen, and intervention. It succinctly describes the spread of a disease in terms of the expected (or average) number of secondary infections that one case of a disease would cause in an otherwise susceptible population [4]. Any intervention that reduces R_0 then reduces the spread of the disease and therefore the final size of the epidemic [5].

However, when relying on R_0 to describe an outbreak, we are using an average to describe a population. Not only are we saying that all individuals are equivalent to an average individual, but also that all contacts are equivalent and equally likely. Often called a *mass-action approximation*, this assumption essentially means that we are considering a randomly mixed population, ignoring household structures, social gatherings and the different behaviors of different individuals. There are obvious mathematical issues in using only the average of a distribution while ignoring the underlying heterogeneity [6]. There are also conceptual issues when relying on these mass-action assumptions to design targeted interventions. Who should we target for an intervention if everyone is equivalent? Where should we target our interventions if all contacts are equal? In this paper, we focus on answering the latter question by examining higher-order contact patterns rather than individuals only.

Network science provides a natural framework to go beyond the mass-action approximation by considering key features of the structure of contacts among individuals. The simplest generalization is perhaps the *heterogeneous pair approximation*—individuals are categorized by their number of contacts, and the contacts themselves by the states of individuals involved. Whereas classic models only track the fraction of susceptible S and infectious I individuals, we now track the proportion of susceptible and infectious individuals with k contacts (S_k and I_k respectively) and the fraction of contacts in the network connecting two susceptible individuals ($[SS]$) or two infectious individuals ($[II]$) or one of each ($[SI]$).

Network representations have had great success because they provide a mathematical perspective on targeted interventions [7]: How much more effective is it to vaccinate nodes of high degree versus random nodes? Simple and efficient targeted intervention strategies, such as acquaintance immunization [8], leverage the friendship paradox [9]: A node reached through a random edge is expected to be more connected and central than a random node. Basically, in heterogeneous systems, an intervention is more likely to reach a well-connected individual if it follows a random contact than if it picks a random individual since well-connected individuals simply have more contacts. That being said, all pairwise contacts are still, a priori, equivalent.

One developing area in network science concerns dynamical processes on higher-order representation of networks, i.e., where the network is not simply a conglomerate of pairwise interactions but where interactions occur in a coordinated manner because of a higher level structure. For example, it is not pure coincidence that many contacts exist among students in a school—these contacts are shaped by a hierarchy of higher level structures of various sizes (groups, classes, sports team, etc.). To explicitly account for this higher-order rep-

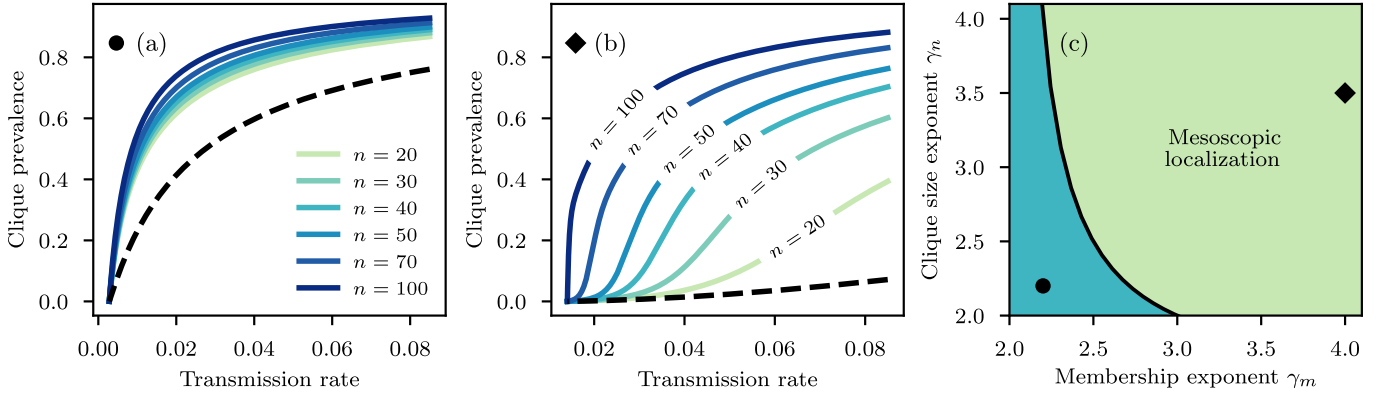


FIG. 1. **Epidemic localization in networks with heterogeneous higher-order structures.** (a)-(b) Solid lines represent the clique prevalence—the average fraction of infectious nodes within cliques of size n —while dashed lines represent the global prevalence. (a) If the structures are highly coupled, we find results in agreement with a mass-action approximation: The fraction of infectious individuals is similar among all of them. (b) With a lower and more realistic coupling between structures, we find a surprising phenomenon of mesoscopic localization. While the global prevalence in the population can remain extremely low, larger structures can self-sustain the epidemic. Smaller cliques are able to self-sustain the epidemic for a more transmissible contagion. (c) Mesoscopic localization is actually the norm rather than the exception. Indeed, the phenomenon is observed for all but the most extremely coupled scenarios when using power-law distributions for the memberships $g_m \sim m^{-\gamma_m}$ and clique sizes $p_n \sim n^{-\gamma_n}$. The solid line separating the *delocalized regime* (blue region) and the *localized regime* (green region) is obtained analytically in Appendix D. The circle and diamond markers correspond to the networks respectively used in panels (a) $\gamma_n = \gamma_m = 2.2$ and (b) $\gamma_n = 3.5, \gamma_m = 4$.

resentation, one straightforward generalization of the framework described in the previous paragraph is the *heterogeneous clique approximation* [10], where we track

1. the proportion of susceptible and infectious individuals with number m of memberships to higher-order structures (S_m and I_m respectively);
2. the fraction of higher level structures containing n members, i of which are infectious ($C_{n,i}$).

As we will now show, even dynamics of simple contagion on these higher-order structures can have surprising features that should prove important for their control.

II. LOCALIZATION

Standard models have a straightforward relationship between the transmission rate of an epidemic (or its R_0) and the expected outbreak size. In Fig. 1, we show the epidemic size of Susceptible-Infectious-Susceptible (SIS) dynamics on a simple version of higher-order network. The network is characterized by g_m , the distribution for the memberships m of nodes and p_n , the distribution for the sizes n of higher level structures. We use different heterogeneous distributions for both and assume that all structures are cliques where every node can transmit the disease to each other.

As expected from standard models, there exists a critical value β_c for the transmission rate β below which epidemics cannot be sustained. This is a typical phase transition, where the disease-free equilibrium of the dynamics becomes unstable above β_c , driving the epidemic to invade the system. Also expected, based on intuition alone, is that larger structures (larger n) likely contain more infectious individuals than

smaller ones. From a mass-action perspective, the fraction of infectious individuals would be similar among all structures, which is approximately what we observe in Fig. 1(a).

What is less expected are the sequential local transitions observed in the second panel [Fig. 1(b)]. For any value of the transmission rate, the outbreak appears to thrive only in structures above a certain size—the epidemic is *self-sustained* locally. This is reminiscent of certain infections, such as the bacteria *C. difficile*, which are most commonly found in settings with large susceptible populations in close contact, like hospitals [11]. Such infections only survive in these dense, vulnerable, social structures.

Any outbreak in a finite size structure left alone would eventually go extinct as the disease-free equilibrium is always an absorbing state. It is therefore the coupling across cliques that allows the epidemic to localize around many large but finite structures. Moreover, through the same mechanism as the friendship paradox described above, the individuals found in a given clique belong to more structures than the average individual. Therefore, large and dense structures have the twofold effect of containing many individuals, and these individuals tend to be more active through a *higher-order friendship paradox*. It is through this size and coupling effects that the epidemic can thrive and self-sustain only in specific structures within the population.

Perhaps most surprising is how strong this localization effect can be. Even at low overall prevalence, the localization of the outbreaks causes intense but local outbreaks in large structures. This simple observation justifies the potential need for school closures and canceling large social or professional events. While it may seem like an overreaction given the low prevalence found in the general population, these dense structures are where most infections will occur.

III. INTERVENTION

Interventions such as school closure or cancellation of large gatherings can be modeled by simply forcing a hard cut-off n_{\max} on the size distribution of structures p_n found in a network. In Fig. 2, we again show the local prevalence within certain structures but only after having removed all structures above n_{\max} .

In the delocalized regime [Fig. 2(a)] where a disease is found throughout a population, the intervention mostly appears to reduce individual risk of infections. As we decrease n_{\max} (and therefore increase the intensity of the intervention), the local prevalence within structures all decrease gradually until an epidemic threshold. This is akin to classic models where the intervention simply reduces R_0 in a distributed, mass-action, way [12].

In the localized regime [Fig. 2(b)] where a disease can self-sustain only around certain structures, the intervention has a totally different impact. Some individuals that would have interacted in structures of size greater than n_{\max} are spared, but large structures of size just below n_{\max} appear unaffected by the intervention. However, there seems to exist a critical cut-off $n_c = 23$ where the intervention is now strong enough to cause a global collapse of the epidemics across all structures.

The key point here is that if an epidemic can self-sustain only around certain structures (e.g. mass transit in urban centers, larger gatherings, cruise ships), an intervention that affect other structures will not affect the local outbreak. Unless, of course, the intervention is strong enough to remove the coupling across large structures where the epidemic is localized.

We also compare the global impact of interventions in the two regimes in Fig. 2(c). These results clarify two things. First, even if a weak intervention does not affect the prevalence in cliques where the epidemic is self-sustained, it does affect global prevalence: It reduces the total disease burden by sparing individuals who would have been infected through spillover transmission from larger cliques. Second, the critical extinction of the outbreak observed in Fig. 2(b) when removing cliques larger than n_c is due to increasing returns in the effectiveness of the intervention. In standard, delocalized dynamics, we see a linear relationship between the outbreak size and the strength of the intervention, measured in number of contacts avoided. In localized dynamics, we see a non-linear feedback because 1) we are removing structures able to self-sustain themselves and 2) we reduce the coupling across these local outbreaks.

Altogether, the lesson from Fig. 2 is that, just as we take heterogeneity of individual risks into account when preferentially vaccinating some individuals, we should take heterogeneity of structural risks into account when designing interventions that operate on higher-order structures. Since we can expect real epidemics to experience localizations effects, we should try to leverage as much as possible the non-linear feedback [Fig. 2(c)] when cancelling gatherings up to a certain size.

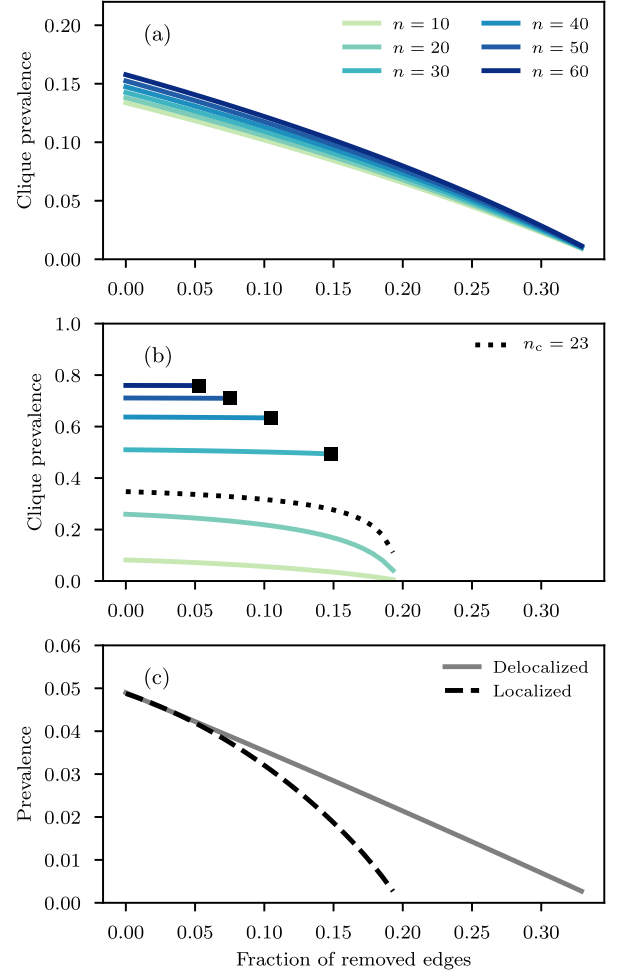


FIG. 2. Structural interventions, such as event cancellations, in delocalized and localized epidemics. (a)-(b)-(c) Prevalence (within structures and globally) against the fraction of potential contacts removed (edges in the network) following an intervention. The intervention removes all cliques of size $n > n_{\max}$. The transmission rate is adjusted to have a similar global prevalence for both regimes without intervention. We used the same networks as in Fig. 1. (a) In the delocalized regime, using a transmission rate $\beta \approx 0.0041$, we find a similar benefit of the intervention among all structures. (b) In the localized regime, using a transmission rate $\beta = 0.07$, we find a different story where prevalence within large structures is barely affected by our intervention, up to a critical cut-off $n_{\max} = n_c$ (here $n_c = 23$) where prevalence within all cliques abruptly falls to zero. Square markers indicate when structures of a particular size are removed. (c) To have a closer look at the importance of structural interventions in the localized regime, we compare the global prevalence in both regimes. We note the increasing returns on interventions in the localized regime, leading to a sudden collapse of the outbreak.

IV. DISCUSSION

Over the last few years, dynamics on higher-order representation of networks have shown time and time again that intuition built from simpler models does not always hold in more complex scenarios, with example ranging from competitive dynamics [13] to social contagion [14]. Localization of

simple epidemic dynamics over higher-order structures is yet another example. While a virus might operate at the scale of individuals, infecting one person after the other, epidemics themselves interact with our entire social structure. We often think in terms of individual risks because that is the scale at which most preventive measures operate, but ignoring higher-order structures would be a mistake when considering interventions that work at a larger scale.

There are some key assumptions built into our model that influence epidemic localization. One major assumption is that we ignore temporal variations in structures. If a structure of size 500 is meant to represent an academic conference, it only takes place over a well-defined period of time. Thankfully, the mean-field approach used does not assume that the exact same events with the exact same participants occur for all time, but it does assume that the density of events of a given size (p_n) is stable over time. Similarly, it only assumes that one's membership number m is a fixed level of participation for that individual. However, the structures or events where that individual participates may vary in time. One second important caveat is that the results were obtained by implementing SIS dynamics, where individuals are fully susceptible immediately after recovering from a disease. Although this is but a simplistic model for most actual epidemics, it allows to characterize analytically the localization features of the dynamics. And while epidemics where individuals develop immunity might never actually self-sustain in a finite size structure, localization still occurs in the form of smeared epidemic transitions [15].

Therein lies the importance of theoretical disease modeling: They broaden our understanding of the dynamical behavior one can expect from new outbreaks, even if the models themselves are often disconnected from actual, current outbreaks, and impossible to parametrize with any available data. We never know when a better understanding of the complex dynamics of epidemics on complex networks will lead to actionable results. In fact, no epidemics are ever alike. We need diversified theoretical models and a deep understanding of their dynamics.

In terms of the current COVID-19 outbreak, it is important to keep in mind that large gatherings can have significantly higher risk than one would believe based on the global prevalence alone. Once we consider the possibility for localized outbreaks, it then makes sense to leverage the results describe above and target our interventions on large higher-order structures. The goal being to decouple structures and cause a rapid collapse of the epidemic. How do we achieve this without a clear intervention from the top? Follow the higher-order friendship paradox: Cancel your next large event [16], and tell your friends to do the same.

ACKNOWLEDGMENTS

L.H.-D. acknowledges support from the National Institutes of Health 1P20 GM125498-01 Centers of Biomedical Research Excellence Award and thanks Simon DeDeo for inspiring him to write this paper. This work was also supported by

the Fonds de recherche du Québec – Nature et technologies (V.T., G.S.), the Natural Sciences and Engineering Research Council of Canada (G.S., V.T., A.A., L.J.D.), and the Sentinel North program of Université Laval, funded by the Canada First Research Excellence Fund (G.S., V.T., A.A., L.J.D.). L.H.-D. also acknowledges the dedication of his ALife 2020 co-organizers, Juniper Lovato and Josh Bongard, in moving the conference online to reduce the spread of COVID-19.

Appendix A: Clique-based SIS model

We consider the SIS model on infinite size random networks with cliques [17]. The network ensemble is characterized by a size distribution p_n for the cliques and a membership distribution g_m for the nodes. Nodes are assigned to cliques uniformly at random, hence there are no correlations between m and n . The transmission rate is β and the recovery rate is set to 1 without loss of generality.

We can describe accurately the dynamics using the heterogeneous clique approximation of Ref. [10]. We want to track $S_m(t)$, the fraction of nodes that are susceptible and of membership $m \in \{1, \dots, m_{\max}\}$ at time t and $C_{n,i}(t)$ the fraction of cliques that are of size $n \in \{2, \dots, n_{\max}\}$ with $i \in \{0, \dots, n\}$ infected nodes at time t . We can factorize g_m and p_n , yielding $s_m(t) \equiv S_m(t)/g_m$, the probability of a node being susceptible given m and $c_{n,i}(t) = C_{n,i}(t)/p_n$ the probability to observe a clique with i infected nodes given n . Omitting explicit time dependency for readability, we use approximate master equations to follow these quantities:

$$\frac{ds_m}{dt} = 1 - s_m - \beta m r s_m, \quad (\text{A1a})$$

$$\begin{aligned} \frac{dc_{n,i}}{dt} = & (i+1)c_{n,i+1} - ic_{n,i} + \beta(n-i+1)\{(i-1) + \rho\}c_{n,i-1} \\ & - \beta(n-i)\{i + \rho\}c_{n,i}. \end{aligned} \quad (\text{A1b})$$

The mean fields $r(t)$ and $\rho(t)$ are defined as follows

$$r(t) = \frac{\sum_{n,i} \beta i(n-i)c_{n,i}(t)p_n}{\sum_{n,i} (n-i)c_{n,i}(t)p_n}, \quad (\text{A2})$$

$$\rho(t) = r(t) \frac{\sum_m m(m-1)s_m(t)g_m}{\sum_m m s_m(t)g_m}. \quad (\text{A3})$$

If we take a random susceptible node within a clique, $r(t)$ is the mean infection rate associated with a random *external* clique (excluding the one we picked the node from) to which it belongs and $\rho(t)$ is the mean excess infection rate caused by all *external* cliques.

The global prevalence (average fraction of infected nodes) is then $I(t) = \sum_m g_m [1 - s_m(t)]$ and the prevalence within cliques of size n is $I_n(t) = \sum_i i c_{n,i}(t)/n$.

Appendix B: Epidemic localization in large cliques

In the stationary state near the epidemic threshold, $\rho \rightarrow 0$. We can thus expand $c_{n,i}$ as $c_{n,i} = h_{n,i}\rho + O(\rho^2)$ where we define

$h_{n,i} \equiv \partial_\rho c_{n,i}|_{\rho \rightarrow 0}$. From Eq. (A1) in the stationary state, we obtain

$$h_{n,i} = \frac{n! \beta^{i-1} (i-1)!}{(n-i)! i!} \quad \forall i > 0,$$

and by definition $h_{n,0} \equiv -\sum_{i>0} h_{n,i}$.

An equivalent representation is the following generating function

$$\begin{aligned} H_n(x) &= \sum_i h_{n,i} x^i, \\ &= h_{n,0} + \frac{1}{\beta} \int_0^\infty u^{-1} e^{-u} [(1 + \beta u x)^n - 1] du. \end{aligned}$$

It is then straightforward to obtain $I_n = H'_n(1)\rho/n + O(\rho^2)$. Performing a saddle-point approximation, we obtain the following asymptotic behavior for large clique sizes n

$$H'_n(1) \sim \begin{cases} \frac{n}{1 - \beta n} & \text{if } \beta < 1/n \\ n \sqrt{2\pi n} (\beta n)^n e^{-n+1/\beta} & \text{if } \beta \geq 1/n \end{cases}. \quad (\text{B1})$$

For $\beta = an^{-1}$ and $a > 1$, this implies $I_n \sim O(n^{1/2} e^{bn})$ with $b > 0$. This means that if we are near the epidemic threshold ($\beta = \beta_c + \epsilon$ and $\epsilon \ll 1$) and for some cliques of size n we have $\beta > 1/n$, then we expect the epidemic to be *localized* within these cliques. More formally, we say that the epidemic is localized near the epidemic threshold when $I_{n_{\max}}/I_2 = O(n_{\max}^{1/2} e^{bn_{\max}})$.

It is worth mentioning that other approaches have been used to assess the localization of contagion processes. A useful and popular measure is the *inverse participation ratio* [18–20]. While it has been used mostly to study *hub* localization, where the disease survive around the largest degree nodes, we would expect similar behavior for mesoscopic localization as describe above.

Appendix C: Epidemic threshold

In the stationary state, Eq. (A3) is a self-consistent equation of the form $\rho = F(\rho)$ and a positive solution to ρ exists if

$$\left. \frac{dF}{d\rho} \right|_{\rho \rightarrow 0} > 1.$$

Hence the epidemic threshold β_c is obtained by solving the implicit equation

$$\frac{\langle m(m-1) \rangle}{\langle m \rangle \langle n \rangle} \beta_c \sum_n p_n \{n H'_n(1) - \partial_x [x H'_n(x)]_{x \rightarrow 1}\} = 1.$$

Rearranging the terms and by using the properties of the incomplete gamma function, this can be simplified to

$$\frac{\langle m(m-1) \rangle}{\langle m \rangle \langle n \rangle} \sum_n p_n \{H'_n(1) - n\} = 1. \quad (\text{C1})$$

Appendix D: Localization regimes

Let us consider heterogeneous distributions $p_n \sim n^{-\gamma_n}$ and $g_m \sim m^{-\gamma_m}$ with $\gamma_n, \gamma_m > 2$ to have finite moments $\langle n \rangle$ and $\langle m \rangle$. We impose finite size effects by introducing a number of nodes N and by considering natural cut-offs [21] for both distributions $n_{\max} \sim N^{1/(\gamma_n-1)}$ and $m_{\max} \sim N^{1/(\gamma_m-1)}$. We can then extract the asymptotic behavior of the epidemic threshold for large N , giving us insights on the type of phase transition expected for different scenarios.

Let us first consider $\gamma_m > 3$. In this case, Eq. (C1) has the following behavior

$$\int_{n_{\min}}^{n_{\max}} n^{-\gamma_n} [H'_n(1) - n] \sim 1.$$

The asymptotic behavior of $H'_n(1)$ for large n will dictate the scaling of the epidemic threshold. According to Eq. (B1), we have two possible asymptotic behaviors. However, only the sub-exponential one for $n_{\max} \rightarrow \infty$ can respect the preceding equation. Therefore, we obtain

$$\int_{n_{\min}}^{n_{\max}} n^{1-\gamma_n} \left[\frac{1}{1 - \beta_c n} - 1 \right] \sim 1.$$

This leads to two possible asymptotic scalings for the threshold

$$\beta_c \sim \begin{cases} n_{\max}^{-1} & \text{if } \beta_c n_{\max} \rightarrow 1 \\ n_{\max}^{\gamma_n-3} & \text{if } \beta_c n_{\max} \rightarrow 0 \end{cases}.$$

However, because of the condition $\gamma_n > 2$, only the first one is admissible. Therefore we have $\beta_c \rightarrow 1/n_{\max}$. This implies that right above the epidemic threshold ($\beta = \beta_c + \epsilon$), we have $I_{n_{\max}}/I_2 = O(n_{\max}^{1/2} e^{bn_{\max}})$ and thus the epidemic is localized.

Let us now consider $\gamma_m < 3$. In this case,

$$\frac{\langle m(m-1) \rangle}{\langle m \rangle} \sim m_{\max}^{3-\gamma_m}.$$

By performing a similar development, we obtain

$$\beta_c \sim \begin{cases} n_{\max}^{-1} & \text{if } \beta_c n_{\max} \rightarrow 1 \\ n_{\max}^{\gamma_n-3} m_{\max}^{\gamma_m-3} & \text{if } \beta_c n_{\max} \rightarrow 0 \end{cases}.$$

If $\beta_c n_{\max} \rightarrow 1$, we again have a localized epidemic. If instead $\beta_c n_{\max} \rightarrow 0$, increasing β just beyond β_c leads to $I_{n_{\max}}/I_2 = O(1)$, and the epidemic is then delocalized. For the natural cut-offs defined above, this happens if

$$4\gamma_n + 3\gamma_m - 2\gamma_n\gamma_m > 5. \quad (\text{D1})$$

This condition clarifies the influence of both exponents on the coupling between cliques, as illustrated in Fig. 1. Equation (D1) was used to distinguish the regimes in Fig. 2(c).

More generally, we do not need to mimic a finite size network, but only need to assume a scaling relationship of the form $m_{\max} \sim n_{\max}^\alpha$. In this case, the epidemic is delocalized if

$$\gamma_n + \alpha(\gamma_m - 3) < 2.$$

As a result, with $\alpha \in [0, \infty)$ and the requirement $\gamma_n > 2$, we see that a minimal condition to have a delocalized epidemic near β_c is $\gamma_m < 3$.

-
- [1] W. O. Kermack and A. G. McKendrick, "Contributions to the mathematical theory of epidemics," *Bull. Math. Biol.* **53**, 33 (1991).
- [2] W. O. Kermack and A. G. McKendrick, "Contributions to the mathematical theory of epidemics. ii - the problem of endemicity," *Bull. Math. Biol.* **53**, 57 (1991).
- [3] W. O. Kermack and A. G. McKendrick, "Contributions to the mathematical theory of epidemics. iii - further studies of the problem of endemicity," *Bull. Math. Biol.* **53**, 89 (1991).
- [4] O. Diekmann, J. A. J. Metz, and J. A. P. Heesterbeek, "The legacy of Kermack and McKendrick," in *Epidemic Model. Their Struct. Relat. to Data*, edited by D. Mollison (Cambridge University Press, 1995) p. 95.
- [5] R. M. Anderson, B. Anderson, and R. M. May, *Infectious Diseases of Humans: Dynamics and Control* (Oxford University Press, 1992).
- [6] L. Hébert-Dufresne, B. M. Althouse, S. V. Scarpino, and A. Allard, "Beyond R_0 : the importance of contact tracing when predicting epidemics," *medRxiv* (2020), 10.1101/2020.02.10.20021725.
- [7] R. Pastor-Satorras and A. Vespignani, "Epidemic spreading in scale-free networks," *Phys. Rev. Lett.* **86**, 3200 (2001).
- [8] R. Cohen, S. Havlin, and D. Ben-Avraham, "Efficient immunization strategies for computer networks and populations," *Phys. Rev. Lett.* **91**, 247901 (2003).
- [9] M. E. J. Newman, *Networks* (Oxford university press, 2018).
- [10] L. Hébert-Dufresne, P.-A. Noël, V. Marceau, A. Allard, and L. J. Dubé, "Propagation dynamics on networks featuring complex topologies," *Phys. Rev. E* **82**, 036115 (2010).
- [11] L. V. McFarland and W. E. Stamm, "Review of clostridium difficile—associated diseases," *Am. J. Infect. Control* **14**, 99 (1986).
- [12] B. F. Maier and D. Brockmann, "Effective containment explains sub-exponential growth in confirmed cases of recent covid-19 outbreak in mainland china," *arXiv preprint arXiv:2002.07572* (2020).
- [13] J. Grilli, G. Barabás, M. J. Michalska-Smith, and S. Allesina, "Higher-order interactions stabilize dynamics in competitive network models," *Nature* **548**, 210 (2017).
- [14] I. Iacopini, G. Petri, A. Barrat, and V. Latora, "Simplicial models of social contagion," *Nat. Commun.* **10**, 1 (2019).
- [15] L. Hébert-Dufresne and A. Allard, "Smeared phase transitions in percolation on real complex networks," *Phys. Rev. Research* **1**, 013009 (2019).
- [16] Or better yet, propose an alternative such as an online version of the event [22].
- [17] M. E. J. Newman, "Properties of highly clustered networks," *Phys. Rev. E* **68**, 026121 (2003).
- [18] A. V. Goltsev, S. N. Dorogovtsev, J. G. Oliveira, and J. F. F. Mendes, "Localization and spreading of diseases in complex networks," *Phys. Rev. Lett.* **109**, 128702 (2012).
- [19] C. Castellano and R. Pastor-Satorras, "Relating Topological Determinants of Complex Networks to Their Spectral Properties: Structural and Dynamical Effects," *Phys. Rev. X* **7**, 41024 (2017).
- [20] R. Pastor-Satorras and C. Castellano, "Eigenvector localization in real networks and its implications for epidemic spreading," *J. Stat. Phys.* **173**, 1110–1123 (2018).
- [21] M. Boguñá, R. Pastor-Satorras, and A. Vespignani, "Cut-offs and finite size effects in scale-free networks," *Eur. Phys. J. B* **38**, 205–209 (2004).
- [22] O. Reshef, I. Aharonovich, A. Armani, S. Gigan, R. Grange, M. A. Kats, and R. Sapienza, "How to organize an online conference," *arXiv preprint arXiv:2003.03219* (2020).